EC
Journals.ASM.org

Activation of an Essential Calcium Signaling Pathway in *Saccharomyces cerevisiae* by Kch1 and Kch2, Putative Low-Affinity Potassium Transporters

Christopher P. Stefan,[a] Nannan Zhang,[a] Takaaki Sokabe,[b] Alberto Rivetta,[c] Clifford L. Slayman,[c] Craig Montell,[b] Kyle W. Cunningham[a]

Department of Biology, Johns Hopkins University, Baltimore, Maryland, USA[a]; Departments of Biological Chemistry and Neuroscience, Center for Sensory Biology, The Johns Hopkins University School of Medicine, Baltimore, Maryland, USA[b]; Department of Cellular and Molecular Physiology, Yale School of Medicine, New Haven, Connecticut, USA[c]

In the budding yeast *Saccharomyces cerevisiae*, mating pheromones activate a high-affinity Ca^{2+} influx system (HACS) that activates calcineurin and is essential for cell survival. Here we identify extracellular K^+ and a homologous pair of transmembrane proteins, Kch1 and Kch2 (Prm6), as necessary components of the HACS activation mechanism. Expression of Kch1 and especially Kch2 was strongly induced during the response to mating pheromones. When forcibly overexpressed, Kch1 and Kch2 localized to the plasma membrane and activated HACS in a fashion that depended on extracellular K^+ but not pheromones. They also promoted growth of *trk1 trk2* mutant cells in low K^+ environments, suggesting they promote K^+ uptake. Voltage-clamp recordings of protoplasts revealed diminished inward K^+ currents in *kch1 kch2* double-mutant cells relative to the wild type. Conversely, heterologous expression of Kch1 in HEK293T cells caused the appearance of inwardly rectifying K^+ currents. Collectively, these findings suggest that Kch1 and Kch2 directly promote K^+ influx and that HACS may electrochemically respond to K^+ influx in much the same way as the homologous voltage-gated Ca^{2+} channels in most animal cell types.

Ca^{2+} is a key messenger that helps translate extracellular stimuli to intracellular responses. Controlled increases in cytosolic free Ca^{2+} concentrations ($[Ca^{2+}]$cyt) regulate numerous processes, including membrane fusion, cytoskeleton organization, gene transcription, cell polarization, and cell death. *Saccharomyces cerevisiae* cells elevate $[Ca^{2+}]$cyt using Ca^{2+}-selective channels that then activate an evolutionarily conserved signaling pathway that involves calmodulin, calmodulin-dependent protein kinases, and calmodulin-dependent protein phosphatases (calcineurin [Cn]), most of which are highly expressed in mammalian cells (reviewed in reference 1).

Increases in $[Ca^{2+}]$cyt and the resulting activation of Cn are essential for survival of *S. cerevisiae* cells responding to mating pheromones (2). Haploid cells can propagate with either **a** or α mating types, and they secrete peptide mating pheromones, **a**-factor or α-factor, to coordinate the mating process (3). Enhanced Ca^{2+} influx through the low-affinity Ca^{2+} influx system (LACS) and the high-affinity Ca^{2+} influx system (HACS) begins approximately 40 min after pheromone stimulation (4, 5). LACS is active in rich media and depends upon a transmembrane protein that resembles the regulatory TARP-subunits of ionotropic glutamate receptors in mammalian cells (6). HACS is active in both rich and synthetic media and is usually required for survival of yeast cells during prolonged exposures to mating pheromones (5). Similar to HACS-deficient mutants, calmodulin- and Cn-deficient cells slowly die when exposed to mating pheromones in the absence of mating partners (2, 5, 7–11). This calcium signaling network therefore regulates cell death in response to stresses induced by mating pheromones. The homologous calcium network in pathogenic yeasts and molds also regulates cell death in response to endoplasmic reticulum (ER) stresses and azole-class antifungals (12).

In *S. cerevisiae*, HACS has been defined by three interacting proteins—Cch1, Mid1, and Ecm7—which are homologous or analogous to subunits of mammalian L-type voltage-gated Ca^{2+} channels (10, 11, 13–15). Cch1, the homolog of the catalytic α_1-subunit of voltage-gated Ca^{2+} channels (VGCCs), contains positively charged residues within its putative voltage-sensing S4 segments (10, 11), suggesting that HACS, too, may be regulated by membrane depolarization. Indeed, a sudden rise of extracellular pH, which is thought to depolarize *S. cerevisiae* cell membranes (15, 16), leads to rapid activation of HACS and elevation of $[Ca^{2+}]$cyt. Hyphal cells of the yeast *Candida albicans* also utilize Cch1 for responses to electrical stimuli (17). However, coexpression of Cch1 and Mid1 from the fungus *Cryptococcus neoformans* in HEK293 cells produced currents that were largely insensitive to voltage in the narrow range tested (18). Therefore, it is not yet clear whether physiological HACS activation in fungi involves membrane depolarization.

S. cerevisiae cells grow best in acidic media, and they employ an electrogenic H^+-ATPase for pH homeostasis and maintenance of a large resting voltage, estimated to be close to −200 mV (19–21). K^+ also contributes to the resting membrane voltage (22, 23), and K^+ uptake by proliferating *S. cerevisiae* cells largely depends on the related K^+ transporters Trk1 and Trk2 (24). In addition, whole-cell patch recordings from protoplasts of *trk1 trk2* mutant cells have demonstrated an ensemble of additional K^+-permeable "channels" that can be blocked by divalent cations (25, 26). Although not formally proved to function as ion channels and not yet identified at the molecular level, these low-affinity transporters

Received 23 October 2012 **Accepted** 26 November 2012
Published ahead of print 30 November 2012
Address correspondence to Kyle W. Cunningham, kwc@jhu.edu.

doi:10.1128/EC.00299-12

TABLE 1 Yeast strains used in this study[a]

Strain	Description or genotype	Source or reference
K432	*bar1*::*hisG*	50
NZY164	*bar1*::*hisG kch2*::*G418*	This study
NZY138	*bar1*::*hisG kch1*::*TRP1*	This study
NZY165	*bar1*::*hisG kch1*::*TRP1 kch2*::*G418*	This study
EMY113	*bar1*::*hisG cch1*::*TRP1*	This study
K601	Wild type	33
CS12	Wild type	This study
CS01	*kch2*::*G418*	This study
CS02	*kch1*::*TRP1*	This study
CS03	*kch1*::*TRP1 kch2*::*G418*	This study
CS04	*cch1*::*HIS3*	This study
CS05	*cch1*::*HIS3 kch2*::*G418*	This study
CS06	*cch1*::*HIS3 kch1*::*TRP1*	This study
CS07	*cch1*::*HIS3 kch1*::*TRP1 kch2*::*G418*	This study
CS30	*trk1*::*LEU2 trk2*::*HIS3*	This study
CS163	*trk1*::*LEU2 trk2*::*HIS3 mid1*::*G418*	This study
CS34	*KCH2-MYC*$_{13}$::*HIS3*	This study
CS83	*KCH1-MYC*$_{13}$::*HIS3*	This study

[a] All of the strains are isogenic derivatives of strain W303-1A (*MAT***a** *ade2-1 can1-100 his3-11,14 leu2-3,112 trp1-1 ura3-1*) and WΔ3 (*trk1*::*LEU2 trk2*::*HIS3* derivative of W303-1A) (22, 23).

TABLE 2 Plasmids used in this study

Plasmid	Description	Source or reference
pJB207	2μ *URA3 FUS1*::*lacZ*	29
pEVP11/AEQ89	2μ *LEU2* P_{ADH}-*aequorin*	30
pSM10	*CEN LEU2* P_{MET25}-HA_3	31
pCS01	*CEN LEU2* P_{MET25}-*KCH2*-HA_3	This study
pCS02	*CEN LEU2* P_{MET25}-*KCH1*-HA_3	This study
pCS42	*CEN URA3* P_{MET25}-HA_3	This study
pCS43	*CEN URA3* P_{MET25}-*KCH2*-HA_3	This study
pCS44	*CEN URA3* P_{MET25}-*KCH1*-HA_3	This study
pEG311	*URA3* P_{TDH3}-*GFP*	51
pCS47	*URA3* P_{TDH3}-*GFP-KCH2*-HA_3	This study
pCS48	*URA3* P_{TDH3}-*GFP-KCH1*-HA_3	This study
pEGFP-C3	P_{CMB}-*EGFP*	Clontech
pCS49	P_{CMB}-*EGFP-KCH2*	This study
pCS50	P_{CMB}-*EGFP-KCH1*	This study

are thought to supply K^+ necessary for the proliferation of *trk1 trk2* double-knockout mutants grown on limiting K^+ (25, 26).

In the present study, we describe two previously uncharacterized proteins, Kch1 and Kch2, which promote low-affinity K^+ uptake and are essential for K^+-dependent activation of HACS in *S. cerevisiae* cells responding to mating pheromones. Both proteins localize to distinct zones of the yeast plasma membrane and are induced during the response to mating pheromones. They also promote cell survival in the presence of mating pheromones. Kch1 and Kch2 therefore define a novel family of fungus-specific proteins that promote K^+ influx and utilization.

MATERIALS AND METHODS

Yeast strains, plasmids, culture media, and reagents. The *S. cerevisiae* strains used in the present study (Table 1) were obtained from original sources or were derived from parental strain W303-1A by means of standard genetic crosses or PCR-based methods for introducing knockout mutations and epitope-tags (27). Yeast strains were cultured in rich yeast extract-peptone-dextrose (YPD) medium or synthetic SC medium (28) and shifted to alternative media as described below. Purified synthetic α-factor mating pheromone was obtained from the Johns Hopkins University Synthesis and Sequencing Facility and was dissolved in dimethyl sulfoxide (DMSO). FK506 was obtained from Astellas Pharma and dissolved in DMSO. Aqueous $^{45}CaCl_2$ was purchased from MP Biosciences.

The plasmids and oligonucleotides used in the present study are listed in Tables 2 and 3. Plasmids pJB207 (*FUS1-lacZ*) and pEVP11/AEQ89 (*ADH-aequorin*) were described previously (29, 30). Genomic *KCH2* and *KCH1* sequences were PCR amplified with linkers, using the forward primers KCH2-PstI-F and KCH1-PstI-F and the reverse primers KCH2-SalI-R and KCH1-SalI-R. They were then digested with PstI and SalI and cloned into pSM10 (31) to yield plasmids pCS01 and pCS02. The *KCH2-HA*$_3$ and *KCH1-HA*$_3$ genes were subcloned into p416MET25 after digestion with SmaI and XhoI to yield plasmids pCS43 and pCS44. HA_3 was subcloned from pSM10 into p416MET25 using SalI and XhoI enzymes, to yield plasmid pCS42. Green fluorescent protein (GFP)-KCH2-HA_3 and GFP-KCH1-HA_3 were PCR amplified from pCS35 and pCS36 using the forward primer MET25(GFP)-BglII-F and the reverse primer MET25(HA_3)-XhoI-R, digested with BamHI and SalI, and then cloned into pEG311 to yield plasmids pCS47 and pCS48. Plasmids pEG311, pCS47, and pCS48 were linearized with BglII before transformation. Genomic *KCH2* and *KCH1* sequences were PCR amplified with linkers using the forward primers KCH2-PstI-F and KCH1-PstI-F and the reverse primers KCH2-XmaI-R and KCH1-XmaI-R and were then cloned into pEGFP-C3 after digestion with PstI and XmaI to yield plasmids pCS49 and pCS50.

$^{45}Ca^{2+}$ uptake assays. Total cellular accumulation of Ca^{2+} was measured as described previously (32). Briefly, yeast cultures were grown to log phase in SC or YPD medium overnight, harvested, and resuspended in fresh SC-100 pH 4 medium spiked with tracer $^{45}CaCl_2$ (Perkin-Elmer) with or without α-factor and FK506, as indicated in figures. SC-100 pH 4 medium was similar to SC medium, except the YNB component was replaced with yeast nitrogen base without calcium and magnesium (Sunrise Scientific Products), the pH was lowered to pH 4.0 using HCl, and the $MgSO_4$ and $CaCl_2$ were restored to 0.5 g/liter and 100 μM, respectively. To maintain selection for plasmids, uracil or leucine were omitted as necessary. The effects of extracellular potassium and sodium and rubidium on Ca^{2+} accumulation were tested by resuspending the log-phase cells in SC-100 pH 4 medium lacking sodium chloride and potassium phosphate and adding solutions of KCl, NaCl, or RbCl to the concentrations indicated in figures. Cultures were then incubated at 30°C in 96-well filtration plates (Millipore MultiScreen HTS plates) or in glass tubes for the specified times, and the cells were harvested by filtration, washed four times with ice-cold buffer A (10 mM $CaCl_2$, 5 mM Na-HEPES [pH 6.5]) on a vacuum filtration unit (Millipore), and dried at room temperature. The filters were covered with Microscint20 scintillation cocktail (Perkin-Elmer), and counted using a TopCount NXT (Packard) or a Tri-Carb 2200 (Packard) liquid scintillation counter. The data were fit to the sigmoidal (variable slope) equation using nonlinear regression (Prism).

Aequorin luminescence measurements. Yeast strains were transformed with the aequorin expression plasmid pEVP11/AEQ89 (30) and grown to log phase in SC minus leucine. Cells (at an optical density at 600 nm [OD_{600}] of 1.0) were harvested, washed, resuspended in SC lacking leucine supplemented with coelenterazine (Molecular Probes), and incubated at room temperature for 30 min. The loaded cells were collected, resuspended in fresh YPD medium, and recovered for 90 min as described previously (5). The cells were then transferred to fresh tubes, incubated at room temperature, read in a tube luminometer (LB9507; EG&G Wallac), and then injected with an equal volume of YPD medium adjusted to pH 10.0 with NaOH while recording luminescence at 0.2-s intervals.

Western blotting. Cultures were grown to log phase at 30°C in YPD medium, adjusted to an OD_{600} of ~0.1, and split into four aliquots. Samples were treated with 1 μg of FK506/ml, 25 μM α-factor, or DMSO control (Sigma-Aldrich) for 3 h at 30°C before processing. Processing

TABLE 3 Oligonucleotides used in this study

Name	Sequence (5′–3′)
KCH2-PstI-F	GACGACCTGCAGATGGAATCAAGTTTACAAAAATTG
KCH2-SalI-R	GACGACGTCGACTATGTATTTATGTTTGTATTTCTG
KCH1-PstI-F	GACGACCTGCAGATGTTTAACCATGATTGGAAGTAC
KCH1-SalI-R	GACGACGTCGACAGTATAATTATATGTACGATCTTC
KCH2-HindIII-R	GACGACAAGCTTTTATATGTATTTATGTTTGTATTTCTG
KCH2-BamHI-F	GACGACGGATCCATGGAATCAAGTTTACAAAAATTG
KCH1-HindIII-R	GACGACAAGCTTTTAAGTATAATTATATGTACGATCTTC
KCH1-BamHI-F	GACGACGGATCCATGTTTAACCATGATTGGAAGTAC
PMET25(GFP)-BglII-F	GACGACAGATCTATGTCTAAAGGTGAAGAATTATTCAC
PMET25(HA3)-XhoI-R	GACGACCTCGAGCTAGCTAGTTCTAGAAGC
KCH2-XmaI-R	GACGACCCCGGGTATGTATTTATGTTTGTATTTCTG
KCH1-XmaI-R	GACGACCCCGGGAGTATAATTATATGTACGATCTTC
KCH2-F1	ATTTTTTACCACATTGTCTAAGAGGGAAAGGAAAATGACAACAAAGCGCTAAATAcggatccccgggttaattaa
KCH2-R1	GAGAATCGATTTACTTTTAATGCATTTTTGCAGTCAAAAAAAGCTTCGTTTACAcatcgatgaattcgagctcg
KCH1-F1	GCAAACACTTTGGTAATTTCATGAATATTTGACTAGCAGGAACAGAAAATCAAAAcggatccccgggttaattaa
KCH1-R1	TTTCTAATCACGTCTATCTAATTCATGAAATATGCAAAGGGCTTTTGCCAGCCTAgaattcgagctcgtttaaac

involved centrifuging 1 OD_{600} unit of cells at 4°C, lysis of cells with trichloroacetic acid, extraction of proteins with sodium dodecyl sulfate (SDS) sample buffer, and then SDS-PAGE and Western blotting as described previously (31). Blots were probed with anti-MYC monoclonal 9E10 antibodies (Covance).

Growth measurements. Yeast strains were transformed with plasmids pCS42, pCS43, and pCS44 and grown overnight to saturation in SC medium lacking uracil and methionine but supplemented with 100 mM KCl. The cells were then harvested, washed twice with distilled water, and resuspended to an OD_{600} of 1. The cells were serially diluted 10-fold in water, and 7 μl of each dilution was spotted onto pH 4.5 SDAP medium (lacking uracil and methionine) in 2% noble agar. The pH 4.5 SDAP medium contained YNB trace elements and vitamins, 2% glucose, 10 mM arginine-HCl buffered to pH 6.5 with phosphoric acid, 200 μM $CaCl_2$, and 200 μM $MgSO_4$, as described previously (25), as well as additional HCl for adjustment to pH 4.5 and either 50 or 100 mM KCl. The plates were photographed after 3 days of incubation at 30°C.

β-Galactosidase assays. To measure the activation of the mating pheromone pathway, yeast strains were transformed with plasmid pJB207 bearing the *FUS1-lacZ* reporter gene and grown overnight to log phase in SC medium lacking leucine. Cells were then harvested and split into pH 4 SC-100 medium containing 0 or 10 mM KCl in the presence or absence of 20 μM α-factor. The cells were incubated at 30°C for 1.5 h and assayed for β-galactosidase activity as described previously (33).

Microscopy. Wild-type yeast strains were transformed with *GFP-KCH1* and *GFP-KCH2* genes under a constitutive promoter and grown overnight to log phase in SC medium. The cells were treated with 10 μM α-factor for 1 h before imaging. HEK293T cells were cultured in Dulbecco modified Eagle medium (Gibco) containing 10% fetal bovine serum, transfected with plasmids pCS49 and pCS50 using Lipofectamine 2000 (Invitrogen), fixed in 4% paraformaldehyde, and stained with DAPI (4′,6′-diamidino-2-phenylindole). Both cell types were imaged on a 510 Meta Confocal LSM (Zeiss) using ×100 and ×40 objective lenses, respectively, and processed using ImageJ.

Electrophysiology of yeast cells. Whole-cell patch-clamp measurements were made on protoplasts of the *kch1 kch2* double-deletion strain NZY165 and its parent strain K432, as previously described (34). Briefly, the strains were grown in liquid YPD medium at 25°C on an orbital shaker, washed twice in 50 mM KH_2PO_4 (pH 7.2) containing 0.2% β-mercaptoethanol, resuspended in the same buffer plus 1.2 M sorbitol and 0.6 U of zymolyase 20T (catalog no. 320921; IMP Biomedicals, Inc., Irvine CA), and incubated with slow rocking for 45 min at 30°C. The resulting protoplasts were spun down at low speed and resuspended in a stabilizing salt solution (220 mM KCl, 10 mM $CaCl_2$, 5 mM $MgCl_2$, and 0.2% glucose, plus 5 mM MES [morpholineethanesulfonic acid] titrated to pH 7.2 with Tris base). With occasional gentle mixing, protoplasts were stable in this suspension for several hours. For use, 2 μl of suspension was pipetted onto the bottom of the recording chamber and allowed to settle for ~10 min, after which the chamber was filled and carefully flushed with a stream of standard recording buffer (150 mM KCl, 10 mM $CaCl_2$, and 5 mM $MgCl_2$, plus 1 mM MES titrated to pH 7.5 with Tris base) to remove debris and nonadherent cells. Patch pipettes were pulled to ~1.5 μm tip diameter from 1.2 mm borosilicate glass, heat-polished to the shape of a pointed dome, and filled with a standard intracellular buffer (175 mM KCl, 1 mM EGTA, 0.15 mM $CaCl_2$ to yield 100 nM free Ca^{2+}, 4 mM $MgCl_2$, and 4 mM K_2ATP titrated to pH 7.0 with KOH). Visibly clean protoplasts ~6 μm in diameter were selected under bright-field illumination (×400) and picked off the chamber bottom by the patch pipette under suction of ~8 cm HO. Gigaseals formed on usable cells within ~5 min and were allowed to stabilize for another 5 to 10 min. Whole-cell recording was obtained via a high-voltage pulse (750 mV, 100 μs) coupled with brief doubling of suction pressure. Control of the voltage-clamp protocol, collection of current data, and preliminary analysis were carried out via an EPC9 amplifier and Pulse software (HEKA Elektronik, Lambrecht, Germany), interfaced with a PowerMac G4 microcomputer. The data were collected at 2 kHz and filtered at 250 Hz.

The control membrane voltage was held at −40 mV, and scans from this level were generated using 2.5-s pulses in 20 mV decrements (range, +20 to −180 mV). Control scans were run in the standard recording buffer, and test scans were run in a similar solution but lacking both $CaCl_2$ and $MgCl_2$ and supplemented with 1 mM EGTA. Averaged currents for all scans at each voltage are shown (see Fig. 6A, left panel) as stacked traces, with negative (downward) currents indicating cation flow from bath to cell interior. Averaged currents for six *kch1 kch2* mutant cells (see Fig. 6A, right panel) were subtracted from the averaged currents for five wild-type cells, thus generating the noisy traces displayed in Fig. 6C. These traces were fitted using IGOR (WaveMetrics, Inc.) to the equation current as follows: $A0 + A1\cdot[1 - \exp(-\alpha1\cdot\text{time})] + A2\cdot[1 - \exp(-\alpha2\cdot\text{time})]$, keeping the reaction constants, α1 and (separately) α2 the same for all six traces. The summary current-voltage plots of Fig. 6B were obtained from grand averages of the last 0.5 s of each averaged trace.

Electrophysiology using HEK293T cells. HEK239T cells were transfected with pEGFP-C3 or pCS50 and cultured for 24 to 36 h. Cells that expressed GFP were subjected to whole-cell patch clamp recordings. The patch pipettes contained a solution of 140 mM KCl, 5 mM EGTA, and 10 mM K-HEPES (pH 7.4). The bath contained either a high divalent K^+ buffer (130 mM KCl, 5 mM $MgCl_2$, 10 mM $CaCl_2$, 10 mM glucose, 10 mM K-HEPES [pH 7.4]) or a low divalent K^+ buffer (130 mM KCl, 1 mM

EGTA, 10 mM glucose, 43 mM mannitol, 10 mM K-HEPES [pH 7.4]). After achieving a whole-cell patch, the membrane potential was initially clamped at −40 mV, and a series of voltage steps from +100 to −120 mV was applied in 20 mV decrements for 1 s. The data were sampled at 10 kHz and filtered at 5 kHz for analysis (Axopatch 200B amplifier with pClamp 10 software; Molecular Devices). Current values at nearly the end of each step pulse were used to plot I-V relationships. All of the values were normalized by cell capacitance (pF) and have been represented as averages ± the standard errors of the mean (SEM). Cells expressing GFP-Kch1 (n = 19) were analyzed on 3 different days, and control samples (n = 9) were analyzed on different days. For cation permeability experiments, the bath contained either a high-divalent Na^+ buffer (130 mM NaCl, 5 mM $MgCl_2$, 10 mM $CaCl_2$, 10 mM glucose, 10 mM K-HEPES [pH 7.4]) or a low-divalent Na^+ buffer (140 mM NaCl, 1 mM EGTA, 10 mM glucose, 10 mM Na-HEPES [pH 7.4]). Voltage ramps (+100 to −120 mV in 3 s) were applied to a whole-cell patch. Reversal potentials were obtained from the I-V plots as the crossing point between the high- and low-divalent buffers both in GFP-Kch1-expressing cells and control cells. The change in reversal potential (ΔV_{rev}) between GFP-Kch1 cells and control cells was used to calculate ion selectivity as follows: $P_{Na}/P_K = \exp(\Delta V_{rev}F/RT)$, where F is the Faraday constant, R is the universal gas constant, and T is the absolute temperature.

Cell death measurements. Cultures were grown overnight to log phase in SC medium at 30°C. At an OD_{600} of 0.1, cells were harvested, resuspended in SC-100 medium containing 25 μM α-factor in the presence or absence of 100 mM $CaCl_2$, and then incubated at 30°C for 7 h in a flat-bottom 96-well dish (Becton Dickinson). For plasmid expression, strains were transformed with plasmids pSM10, pCS01, and pCS02 and grown overnight to saturation in SC medium lacking leucine and methionine. The cells were then diluted back into fresh medium and allowed to recover. After recovery, 50 μM α-factor was added, and the cells were incubated at 30°C for 6 h in a flat-bottom 96-well dish (Becton Dickinson). In both experiments, the preincubated cells (20 μl) were mixed with 180 μl of phosphate-buffered saline containing 1 μg of propidium iodide/ml, and the live and dead cells were counted automatically using a 96-well flow cytometer FACSArray (Becton Dickinson). At least 5,000 cells in each sample were counted.

RESULTS

KCH1 and *KCH2* genes promote HACS activation by physiological stimuli. HACS activity in yeast can be measured by uptake of $^{45}Ca^{2+}$ from the culture medium, and it is particularly strong when Cn-dependent feedback inhibition has been eliminated by the addition of FK506 or other Cn inhibitors (5, 35). Recently, a collection of gene knockout mutants was screened for HACS deficiencies during the responses to two different stimuli: the ER stressor tunicamycin and the mating pheromone α-factor (15). Strong HACS deficiencies were observed in *cch1*, *mid1*, and *ecm7* mutants in both conditions and a reexamination of the data revealed several other mutants with weaker HACS deficiencies. For example, the *prm6* mutant exhibited a partial HACS deficiency in response to α-factor and the *yjr054w* mutant exhibited a partial HACS deficiency in response to tunicamycin. The homologous *YJR054w* and *PRM6* genes, hereafter designated *KCH1* and *KCH2*, respectively, arose from a whole-genome duplication event in an ancestral species of yeast (36) and are predicted to encode closely related transmembrane proteins. To test whether these genes function redundantly in HACS activation and whether the reduced $^{45}Ca^{2+}$ uptake was a consequence of diminished sensitivity to mating pheromones, the single- and double-knockout mutants were reconstructed in the pheromone-hypersensitive W303-1A *bar1* mutant background and assayed for $^{45}Ca^{2+}$ uptake during exposure to α-factor and FK506. Under these conditions, the *kch1* *bar1* mutant behaved similarly to the parent strain, whereas the isogenic *kch2 bar1* double mutant and the *kch1 kch2 bar1* triple mutant exhibited mild and strong HACS deficiencies, respectively (Fig. 1A and B). $^{45}Ca^{2+}$ uptake into the *cch1 bar1* double mutant

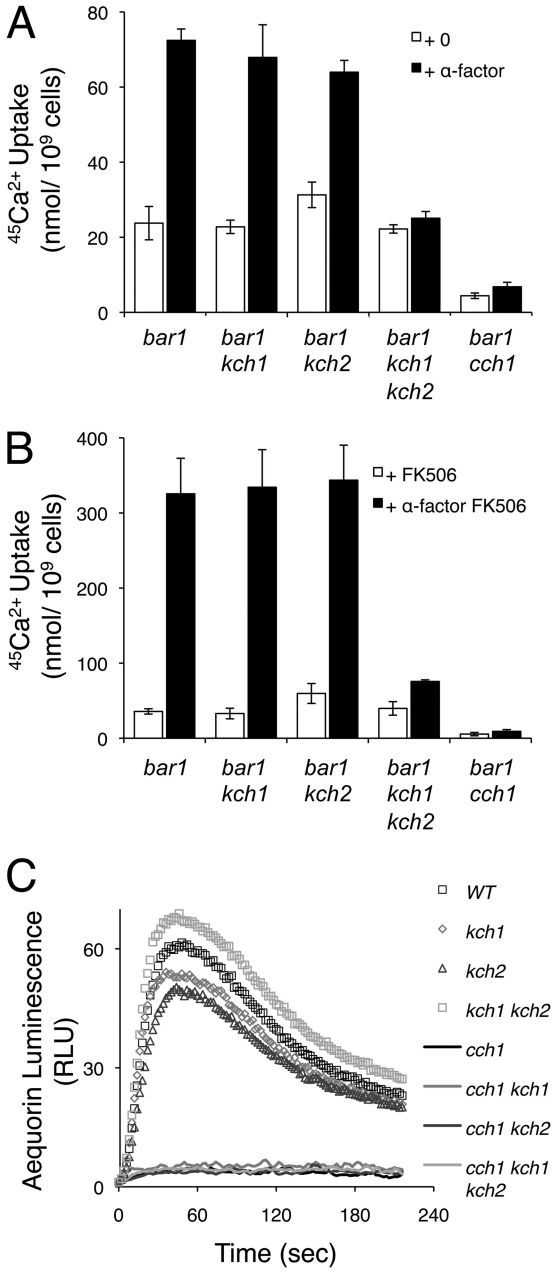

FIG 1 Kch1 and Kch2 regulate HACS activation in response to α-factor mating pheromone. $^{45}Ca^{2+}$ uptake into log-phase cultures of *S. cerevisiae* strains that include combinations of Kch1, Kch2, Cch1, and the secreted protease Bar1 (strains K432, NZY164, NZY138, NZY165, EMY113) was measured after 4 h of incubation in SC-100 medium in the presence or absence of 10 μM α-factor (A) plus 0.2 μg of FK506/ml (B), as indicated. Averages for three biological replicates (± the standard deviations [SD]) are shown. (C) The wild-type strain and *kch1*, *kch2*, and *kch1 kch2* double mutants with or without the functional *CCH1* gene (strains CS12, CS01, CS02, CS03, CS04, CS05, CS06, CS07) all expressing cytoplasmic aequorin from a plasmid (pEVP11/AEQ89) were monitored for luminescence in YPD medium before and after the sudden jump to pH 9.

was slightly less than that of the *kch1 kch2 bar1* triple mutant, indicating a nearly complete loss of the Cn-sensitive HACS activity in the double mutant. These findings suggest that the Kch1 and Kch2 proteins redundantly participate in HACS activation during the response to mating pheromones and not a consequence of desensitization by the Bar1/SstI protease that degrades α-factor.

Sudden elevation of environmental pH causes very rapid activation of HACS and elevation of $[Ca^{2+}]$cyt levels independent of Cn, as detected by measurements of aequorin luminescence (16). Surprisingly, *kch1 kch2* double mutants and both of the single mutants exhibited wild-type levels of aequorin luminescence after high-pH shock (Fig. 1C). The further loss of *CCH1* in these strain backgrounds almost completely eliminated the elevation of $[Ca^{2+}]$cyt (Fig. 1C). Thus, *KCH1* and *KCH2* do not encode essential subunits of HACS but instead encode regulators that are specifically required for HACS activation in response to stimulation with mating pheromones.

Roles of Kch1 and Kch2 in yeast cell death. HACS and Cn are not required for mating and instead are required for the survival of yeast cells that are responding to mating pheromones but unable to find mates (2, 5, 7–11). To determine whether *KCH1* and *KCH2* are also necessary for survival during prolonged episodes of pheromone signaling, cultures of the *kch1 kch2* double mutant and the single mutants were exposed to α-factor and analyzed for dead cells after staining with propidium iodide as described previously (2). Both *kch1* and *kch2* showed low levels of cell death in response to mating pheromone; however, the *kch1 kch2* double mutant exhibited a large increase of cell death (Fig. 2A). Moreover, the pheromone-induced death of the *kch1 kch2* double mutant was suppressed by elevation of extracellular Ca^{2+} concentrations with the addition of 100 mM $CaCl_2$ (Fig. 2A). These conditions allow Ca^{2+} to leak into the cell via other pathways and bypass the necessity of Cch1 and Kch1/2. Overexpression of either Kch1 or Kch2 was able to rescue viability of a *kch1 kch2* double mutant but not a *cch1 kch1 kch2* triple mutant (Fig. 2B). Collectively, these data suggest that Kch1 and Kch2 function upstream of HACS and that cell death in the double mutant results from an inability to take up Ca^{2+} from the extracellular environment and activate the calcium signaling pathway.

Expression, regulation, and localization of Kch1 and Kch2. The products of *KCH1* and *KCH2* were predicted to contain at least two transmembrane spans (38). PSI-BLAST searches of current protein databases revealed homologous proteins encoded in the genomes of nearly all fungi but not in other eukaryotic or prokaryotic species, suggesting a fungus-specific gene family (data not shown). Multiple sequence alignments of representative members of the Kch2 family of proteins revealed strong amino acid sequence conservation within the N-terminal 290 amino acid residues of Kch1 and Kch2, which included all of the predicted transmembrane segments (data not shown). The C-terminal tails were hydrophilic and highly variable in length and sequence. None of the proteins in the Kch1 family have been studied previously.

To study the expression patterns of Kch1 and Kch2, the MYC_{13} epitope tag was inserted at the C termini of these proteins by homologous recombination into the yeast genome. Western blots of whole-cell lysates showed expression of Kch1 and Kch2 proteins to be enhanced in cells exposed to α-factor (Fig. 3A). In the absence of α-factor, basal expression of Kch2 was undetectable. Transcription of the *KCH1* and *KCH2* genes was strongly induced

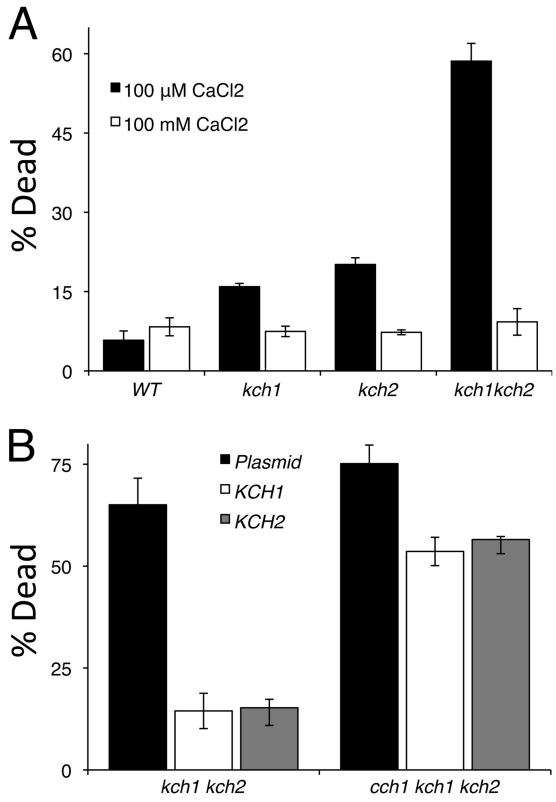

FIG 2 Kch1 and Kch2 are essential for maintaining cell viability. (A) The strains listed in Fig. 1C were exposed to 25 μM α-factor in SC-100 media with or without additional 100 mM $CaCl_2$ and stained with propidium iodide. Live and dead cells were counted by flow cytometry. (B) Strains *kch1 kch2* and *cch1 kch1 kch2* (CS03 and CS07) were transformed with a control plasmid or plasmids that overexpress the *KCH2-HA*$_3$ or *KCH1-HA*$_3$ genes (pSM10, pCS01, and pCS02), exposed to 50 μM α-factor, and then analyzed for pheromone-induced cell death as in panel A. The averages of three biological replicates (± the SD) are shown.

during the response to α-factor (37, 38), which led to the original naming of *KCH2* as pheromone-regulated membrane protein 6 (*PRM6*). The induced Kch1 and Kch2 proteins both migrated as doublets on SDS-PAGE, but changes in their gel mobility and their expression levels were not reproducibly altered by the additional exposure of the cells to FK506. These results suggest that upregulated expression of Kch1 and Kch2 mediates the activation of HACS during the response to mating pheromones and that Cn likely inhibits HACS directly (39) rather than inhibiting Kch1 or Kch2.

To determine the spatial distributions of Kch1 and Kch2 in the cell, the proteins were tagged with GFP at their N termini and overexpressed from a constitutive promoter. Both GFP-tagged proteins were able to prevent cell death when expressed in *kch1 kch2* mutant cells (data not shown), suggesting that fusion proteins were functional. GFP-Kch1 fluorescence was localized to the plasma membrane region of log-phase cells, with a slight enrichment in the growing bud, compared to the mother cell body (Fig. 3B). GFP-Kch2 fluorescence was localized to the distal tip of growing buds and to the vacuole lumen (Fig. 3C). The simplest interpretation of these findings is that Kch2 is initially delivered to sites of cell growth but is subsequently endocytosed and trafficked to the vacuole, likely at different rates from other regions of the

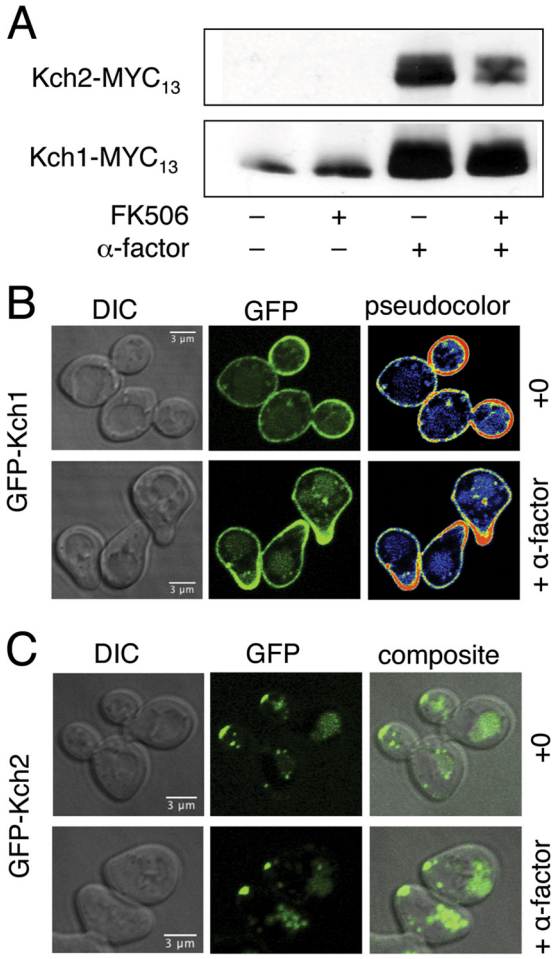

FIG 3 Expression and localization of Kch1 and Kch2 in yeast cells responding to α-factor. (A) Western blots on whole-cell lysates of wild-type yeast strains (K601) expressing Kch2-MYC_{13} and Kch1-MYC_{13} from the chromosomal loci (CS34 and CS83) in the presence or absence of 1 μg of FK506/ml and 25 μM α-factor. Wild-type yeast cells (K601) expressing *GFP-KCH1* (B) and *GFP-KCH2* (C) from constitutive plasmids (pCS47, pCS48) were imaged after exposure to 10 μM α-factor or solvent. Pseudocolored images in panel B depict the scale of pixel intensity.

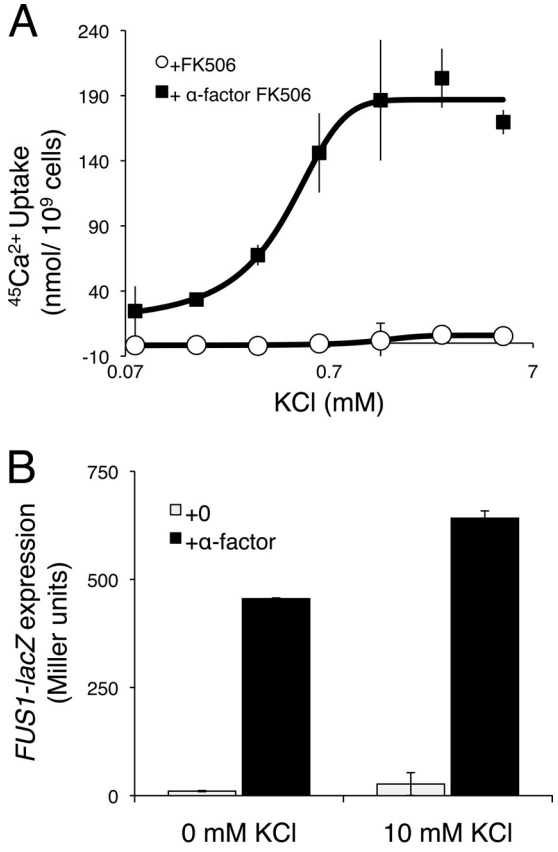

FIG 4 K^+ is essential for the Ca^{2+} accumulation in response to α-factor mating pheromone. (A) Kch1/2-dependent $^{45}Ca^{2+}$ uptake was determined in SC-100 medium containing the indicated concentrations of KCl by subtracting the values obtained from *kch1 kch2* double-mutant cultures (CS03) from those obtained from wild-type cultures (K601) with or without 4 h exposure to 25 μM α-factor plus 0.2 μg of FK506/ml. (B) β-Galactosidase activity of wild-type cells (K601) transformed with a *FUS1-lacZ* reporter gene (pJB207) in SC-100 medium in the presence or absence of 25 μM α-factor and 10 mM KCl. Bars indicate the averages (arithmetic means) of three biological replicates (± the SD).

plasma membrane. This interpretation is supported by a much broader distribution of GFP-Kch2 fluorescence in the plasma membranes of an endocytosis-deficient mutant (*end3* [unpublished observations]). In shmoo-shaped cells responding to α-factor, GFP-Kch1 fluorescence was concentrated in the growing projection, while GFP-Kch2 fluorescence was localized in the tip of the projection as well as in the vacuole lumen.

Kch1 and Kch2 promote K^+ uptake and K^+-dependent activation of HACS. Given the high sequence similarities between Cch1 and the catalytic subunits of mammalian voltage-gated Ca^{2+} channels (10, 11), we supposed that activation of HACS during the response to mating pheromones is likely to involve electrical depolarization of the cell membrane. To test whether HACS activity requires the influx of K^+ or Na^+, we measured $^{45}Ca^{2+}$ uptake into wild-type and *kch1 kch2* mutant yeast cells responding to α-factor and FK506, but in medium lacking these cations. Omission of K^+ and Na^+ from the media resulted in an impairment of HACS activity that could be complemented by the addition of extracellular K^+ (Fig. 4A). However, removal of K^+ did not block other cellular responses to α-factor, such as expression of the pheromone-responsive *FUS1-lacZ* reporter gene (Fig. 4B). Thus, extracellular K^+ was specifically required for HACS activation in response to mating pheromone.

Yeast cells normally accumulate K^+ via two high-affinity transporters, termed Trk1 and Trk2 (24), which are required for proliferation in low-K^+ culture media. Knockout mutations that destroy Kch1 and Kch2 functions did not detectably exacerbate the K^+-requirements of strains lacking Trk1 and Trk2 (data not shown). However, in low-pH media designed to block residual K^+ uptake (25), the overexpression of either Kch1 or Kch2 in *trk1 trk2* double-mutant cells significantly improved the growth relative to controls (Fig. 5A). Similar growth enhancement was also observed in *trk1 trk2 mid1* triple mutants, implying that Kch1 and Kch2 can promote K^+ uptake independently of HACS.

In the absence of mating pheromones and the presence of FK506, the overexpressed Kch1 and Kch2 proteins stimulated $^{45}Ca^{2+}$ uptake in wild-type cells and not in *cch1* mutant cells (Fig.

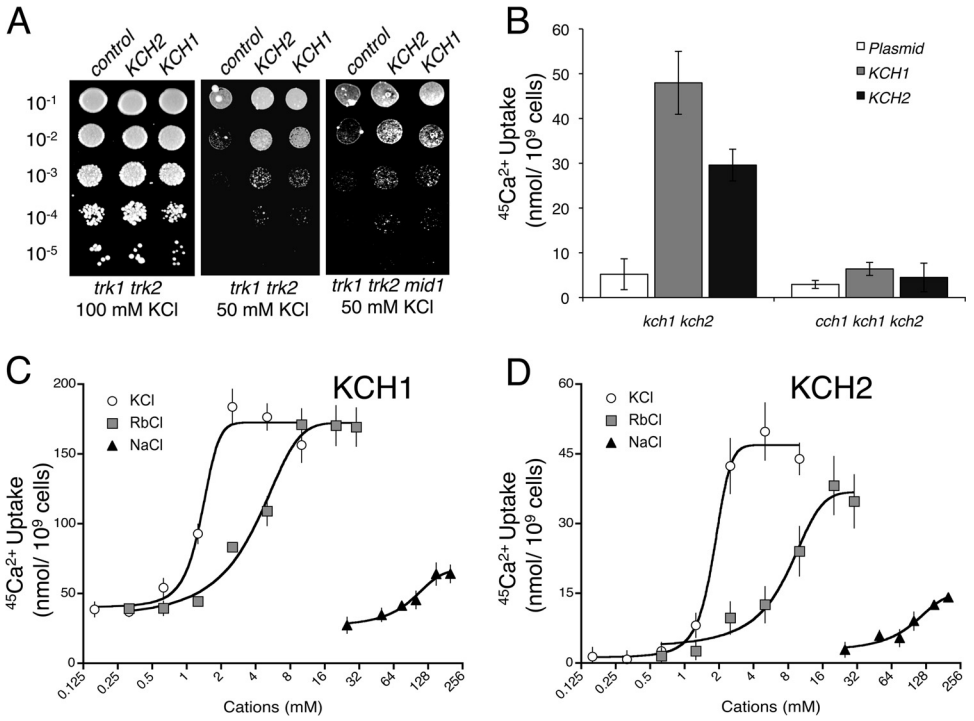

FIG 5 Kch1 and Kch2 promote K^+ uptake and K^+-dependent activation of HACS. (A) A *trk1 trk2* double mutant and a *trk1 trk2 mid1* triple mutant (CS30 and CS163) bearing a control plasmid or plasmids overexpressing *KCH1-HA*$_3$ or *KCH2-HA*$_3$ genes (pCS42, pCS43, and pCS44) were serially diluted and then spotted onto SDAP pH 4.5 agar medium lacking methionine but containing 100 or 50 mM KCl as indicated. Colonies were photographed after 3 days incubation at 30°C. (B) $^{45}Ca^{2+}$ uptake into log-phase cultures of *kch1 kch2* double mutants and *cch1 kch1 kch2* triple mutants (CS03 and CS08) transformed with control plasmid or plasmids overexpressing *KCH1-HA*$_3$ and *KCH2-HA*$_3$ genes, in SC-100 medium supplemented with 1 μg of FK506/ml and incubated for 1.5 h. (C) $^{45}Ca^{2+}$ uptake into the *kch1 kch2* double mutants expressing *KCH1-HA*$_3$ and *KCH2-HA*$_3$ genes was performed in SC-100 media that had been supplemented with 0.2 μg of FK506/ml plus the indicated concentrations of KCl, RbCl, or NaCl. The data points were normalized to corresponding plasmid controls to represent Kch1- and Kch2-dependent calcium uptake. Plots depict averages (± the SEM).

5B). This Kch1- and Kch2-dependent HACS activation was not observed in culture medium depleted of K^+ and Na^+ (Fig. 5C and D). Titration of Na^+, K^+, and Rb^+ salts into the medium demonstrated that K^+ and Rb^+ were 4- to 40-fold more effective than Na^+ at restoring Kch2- and Kch1-dependent activation of HACS. Taken together, these data suggest that Kch1 and Kch2 can mediate the influx of K^+ from the external environment and that this K^+ influx is essential both for the activation of HACS and for the accumulation of Ca^{2+}.

Kch1 and Kch2 define a novel family of K^+ transporters. *S. cerevisiae* cells display a variety of inwardly rectified cation currents, dubbed NSC currents (25, 26), that have not been identified at the molecular level. To determine whether Kch1 and Kch2 might contribute to these currents, the *kch1 kch2* double-knockout strain and the wild-type parent strain were grown under standard conditions, protoplasted, and analyzed by whole-cell patch-clamping (see Materials and Methods). The *kch1 kch2* mutant cells exhibited inward K^+ currents at negative membrane voltages that were only ~40% of the currents in wild-type cells. This can be seen by comparing either the individual downward traces in Fig. 6A or the averaged steady-state values (plotted against membrane voltage) in Fig. 6B. Figure 6A also demonstrates that the amplitudes of the two sets of currents evolved differently in time. The implied *difference* tracings are shown against an expanded ordinate scale, in Fig. 6C, where they have been fitted (smooth red curves) by the sum of two simple exponential functions plus an offset (see Materials and Methods). The same rate constants—7.73/s and 0.21/s (corresponding to half times of 0.09 and 3.27 s)—satisfied all six tracings. The *kch1 kch2* double-mutant cells appeared to lack the faster evolving current. These findings show that Kch1 and Kch2 are necessary components of NSC currents in *S. cerevisiae* and that additional unidentified K^+-permeable channels or transporters also exist.

To test the hypothesis that Kch1 and Kch2 directly promote K^+ flux through the membrane, we expressed the GFP-Kch1 and GFP-Kch2 fusion proteins in human HEK293T cells and carried out whole-cell voltage-clamp measurements. GFP-Kch1 clearly localized to the cortex of HEK293T cells (Fig. 7A), whereas GFP-Kch2 primarily localized to punctae within the cell bodies and was not studied further. At −120 mV, the average inward current in the cells expressing GFP-Kch1 (34.9 ± 7.5 pA/pF; $n = 19$) was significantly higher than that of control cells (13.5 ± 2.6 pA/pF; $n = 9$). Similar to the total inward K^+ currents in wild-type *S. cerevisiae* cells (Fig. 6C), the Kch1-dependent currents in HEK293T cells exhibited inward rectification (Fig. 7D) and were blocked by divalent cations in the bath (Fig. 7C). In addition, the Kch1-dependent currents in HEK293T cells were equally permeable to Na^+ versus K^+ ($P_{Na}/P_K = 1.088$), suggesting that Kch1 induces nonselective cation channels in these assay conditions. Collectively, the findings support a model where Kch1 directly functions as a K^+-permeable transporter or channel in *S. cerevi-*

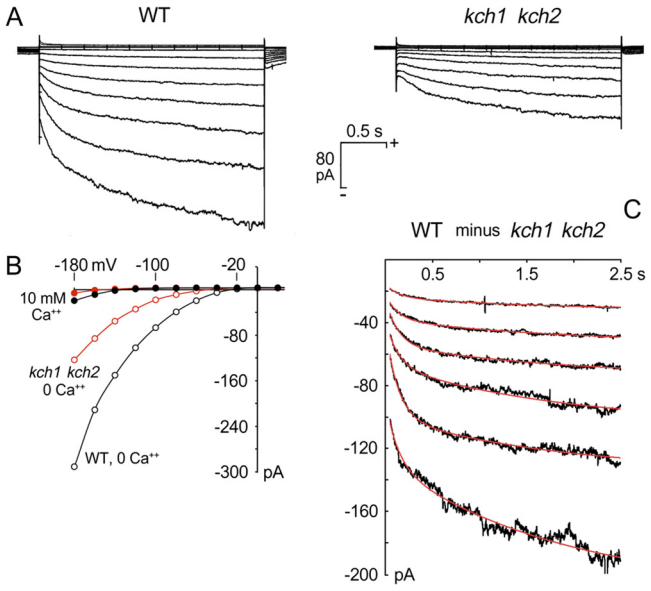

FIG 6 Kch1 and Kch2 mediate inward K^+ currents. (A) Averaged patch-clamp traces from protoplasts of the wild-type strain (K432, $n = 5$, left panel) and the *kch1 kch2* double mutant (NZY165, $n = 6$, right panel), recorded after 10 min incubation in Mg^{2+}- and Ca^{2+}-free recording buffer (see Materials and Methods). (B) Current-voltage plots for the steady-state currents from panel A, plus controls obtained from the same protoplasts, but with 10 mM extracellular Ca^{2+}. Steady-state values calculated from the grand average data, over the interval 2.0 to 2.5 s, along each trace. (C) Plotted differences between corresponding traces of the two panels in panel A. These difference curves are well fitted by the sum of two simple exponentials plus an offset (see equation in Materials and Methods), with the same pair of rate constants for all six plots: $\alpha 1 = 7.725$ s, and $\alpha 2 = 0.212$ s, corresponding to half times of 90 ms and 3.27 s, respectively.

siae with physiological roles in the stimulus-dependent activation of HACS.

DISCUSSION

The evidence presented here suggests that Kch1 and Kch2 activate HACS and downstream components of the essential calcium signaling pathway in *S. cerevisiae* cells during the response to mating pheromones through their ability to transport K^+, likely through the partial depolarization of the plasma membrane. The maintenance of Kch1-related proteins and Cch1-related proteins in most other fungal species suggests that fungi in general may utilize membrane depolarization in the regulation of HACS activity, similar to the mechanism by which mammalian cells regulate VGCCs. These findings and their implications are discussed below in more detail.

Kch1 and Kch2 define a novel family of ion transporters in fungi. Most K^+ uptake in *S. cerevisiae* occurs via the high-affinity and moderate-affinity K^+ transporters Trk1 and Trk2 (24). Mutant cells that lack both Trk1 and Trk2 fulfill their nutritional requirements for K^+ using an ensemble of unidentified low-affinity K^+ uptake systems that can be distinguished electrophysiologically by their rates of evolution after voltage changes (e.g., instantaneous, fast, and slow components), their permeability to Li^+, and sensitivities to other inhibitors (25, 26). Kch1 and Kch2 were specifically required for the fast-evolving K^+ influx current in *S. cerevisiae* cells (Fig. 6). The residual K^+ currents in *kch1 kch2* cells closely resembled the Li^+ currents in wild-type cells (25, 26), suggesting that Kch1 and Kch2 may be incapable of promoting Li^+ transport. Consistent with this view, neither overexpression nor loss of Kch1 and Kch2 in *S. cerevisiae* altered sensitivity to Li^+ in the medium (data not shown). Overexpressed Kch1 and Kch2 also promoted growth of *trk1 trk2* double mutants in limiting concentrations of K^+ in acidic medium (Fig. 5A). Importantly, Kch1 and Kch2 cannot be the sole sources of K^+ uptake because *kch1 kch2 trk1 trk2* quadruple mutants exhibited the same K^+ requirements as the *trk1 trk2* double mutants (unpublished observations) and because the *kch1 kch2* double mutant still retained significant K^+ currents (Fig. 6). Our further observation that Kch1 can generate K^+ currents in HEK293T cells that have selectivity, inhibitor sensitivity, and rectification properties resembling the Kch1/2-dependent currents in *S. cerevisiae* argues strongly that Kch1 and Kch2 can function as the catalytic subunit of ion transporters or channels. However, more experiments will be necessary to rule out the remote possibility that Kch1 regulates an unidentified K^+ transporter that is conserved in both *S. cerevisiae* and human cells.

Kch1 and Kch2 exhibit strong sequence similarity to one another and to uncharacterized proteins present in most other fungi. No homologs of this family can be found in animals, plants, or other eukaryotic species. Many K^+ channels of bacteria and eukaryotes function as oligomers of subunits that have two or six transmembrane segments with a conserved ion selectivity filter located between the final two transmembrane segments (40). The yeast Trk1 and Trk2 K^+ transporters contain four internal repeats of the minimal channel domain present in the homotetrameric KcsA channels of *Streptomyces lividans* (41). Tok1, a bona fide, outwardly rectifying K^+ channel in yeast, appears to form a dimer of subunits that contain two internal repeats of the channel domain (42–44). Each of these K^+ channel domains contains a TVGYG-related sequence that helps form the ion selectivity filter (41, 45). Kch1 and its homologs in other fungi do not contain any TVGYG-related sequence motifs or any other conserved motifs that would be indicative of channel or transporter activity. A better understanding of the transmembrane topology, the oligomeric states, the hypothetical selectivity filter, the transport and gating kinetics, and the regulatory regions of Kch1 and Kch2 will help resolve the means by which this novel family of proteins promotes K^+ influx into fungal cells.

Activation of HACS by Kch1 and Kch2. We first identified *kch1* and *kch2* mutants in a functional screen for genes that were required for activation of HACS in response to mating pheromones and ER stress (15). We show here that mating pheromones induced expression of both Kch1 and Kch2 and overexpressed Kch1 and Kch2 localized to the plasma membrane and activated HACS independent of pheromone stimulation. Thus, Kch1 and Kch2 play crucial roles in HACS activation by mating pheromones. In addition, extracellular K^+ was required for HACS activation in these conditions, although higher concentrations of Rb^+ and Na^+ could partially replace K^+ (Fig. 5). The apparently strong preference for K^+ over Na^+ was not observed in electrophysiological recordings of unstimulated *S. cerevisiae* protoplasts or in HEK293T cells expressing Kch1. This discrepancy may be attributed to several factors. First, the HACS activity assays are performed in standard culture media rather than simple buffers, and therefore represent a more physiological state where additional factors or posttranslational modifications may promote ion discrimination. The ability of Trk1 to discriminate K^+ and Na^+ dramatically depends on signaling pathways that respond to environ-

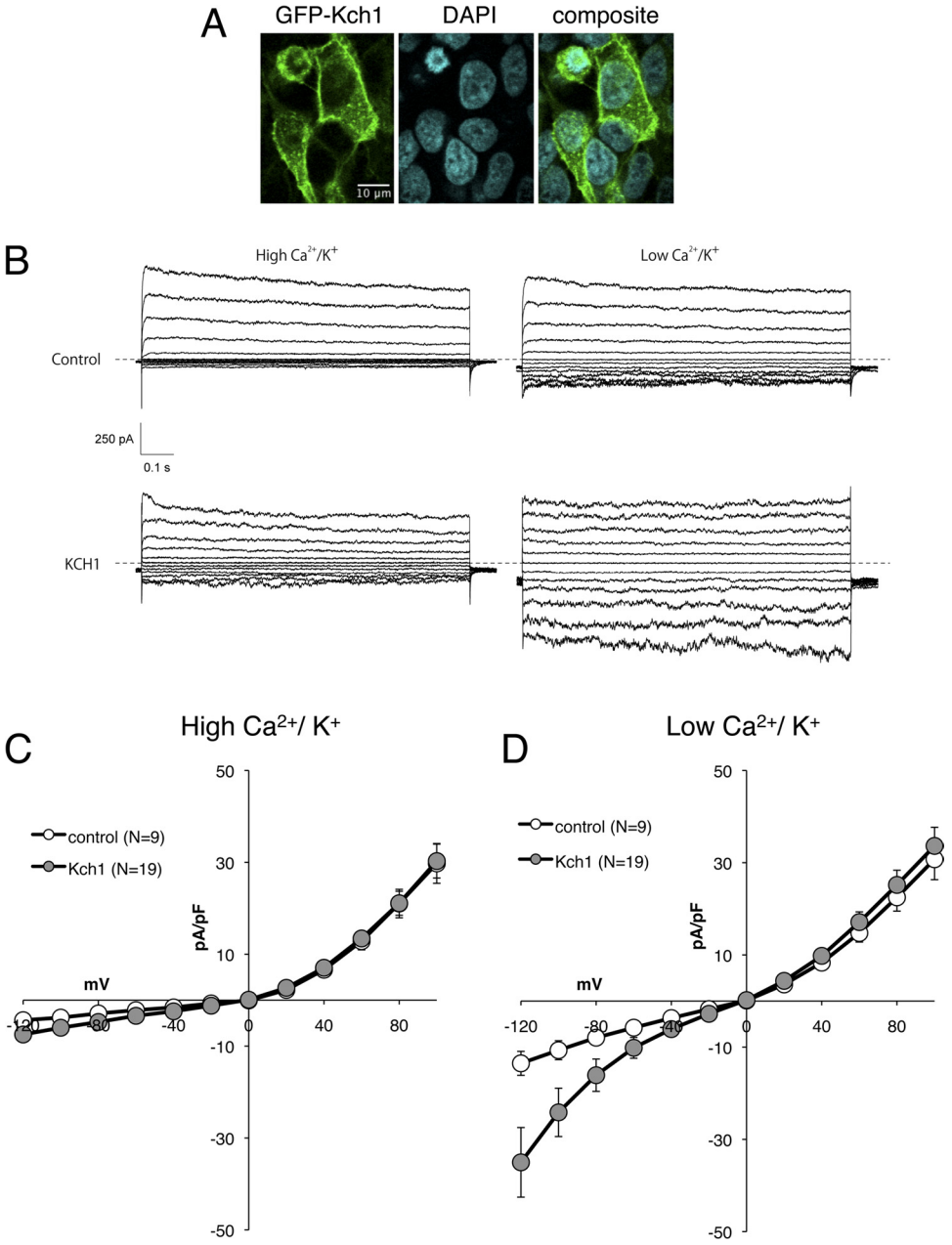

FIG 7 Heterologous expression of Kch1 in HEK293T cells induces inward K^+ currents. (A) HEK293T cells transfected with the *GFP-KCH1* gene (pCS50) were fixed, stained with DAPI, and imaged microscopically. (B) Representative traces of HEK293T cells transfected with plasmid or plasmid containing *GFP-KCH1* gene (pEGFP-C3 and pCS50) subjected to whole-cell voltage-clamp measurements in buffers containing high- or low-divalent cations. (C and D) Current voltage traces summarizing raw data in panel B in high (C)- or low (D)-divalent cation buffers. The plots show averages (± the SEM) of 9 control cells (white symbols) and 19 GFP-Kch1 expressing cells (gray symbols) after normalization with the whole-cell capacitance.

mental conditions (46). Second, K^+ and Na^+ may differentially couple to the activation of HACS through either chemical or electrical intermediates.

The catalytic subunit of HACS, Cch1, is homologous to VGCCs of mammals that are responsive to changes in transmembrane electrical potential through effects on four repeated voltage-sensing domains (47). Mammalian VGCCs generally contain 19 positioned lysine and arginine in the voltage sensing "S4" domains, whereas Cch1 and its homologs in fungi typically contain 11 to 12 lysine and arginine residues at these sites (10, 11, 18), potentially altering the speed and sensitivity of their responses to changes in membrane voltage. Cch1-dependent ion currents have not yet been directly recorded in *S. cerevisiae* or other fungi. After coexpression of Cch1 and Mid1 homologs from the fungus *Cryptococcus neoformans* in HEK293 cells, a Ca^{2+}-selective channel was recorded, but these currents were largely insensitive to voltages within the narrow range tested (−80 to +70 mV) (18). It is possible that voltage sensitivity of this HACS-like fungal channel would be observed at more physiological membrane potentials for fungi (approaching −200 mV) or when the cells coexpress the

regulatory γ-subunit, which was recently identified in *S. cerevisiae* (15). Interestingly, the reconstituted Cch1-Mid1 channel from *C. neoformans* became voltage sensitive when Ba^{2+} was substituted for Ca^{2+} as the charge carrier (18), potentially indicating some feedback regulation by Ca^{2+}. Although there is no direct evidence that fungal HACS channels sense and respond to membrane depolarization, sudden dissipation of the transmembrane H^+ gradient led to rapid activation of HACS in *S. cerevisiae* (16) and *C. albicans* (48) in a fashion that bypassed the requirement for Kch1 and Kch2 (Fig. 1). Although we cannot rule out the possibility that Kch1 and Kch2 activate HACS by more complex mechanisms, the simplest interpretation of the available data is that Kch1 and Kch2 activate HACS via electrical depolarization of the yeast plasma membrane associated with K^+ influx.

K^+ plays a definite role in regulating the resting membrane voltage of yeast, as reflected by the relative hyperpolarization of the plasma membrane in *trk1 trk2* mutants and by the relative depolarization of *tok1* mutants (22, 23). It is therefore consistent that pheromone-dependent induction of Kch1 and Kch2 expression should promote K^+ influx with partial depolarization of the plasma membrane. Until now, there has been no direct evidence of either enhanced K^+ uptake or membrane depolarization during the response to mating pheromones. Early studies failed to detect any significant effect of α-factor exposure on the uptake of Rb^+ as a surrogate for K^+ (4), but the activities of Kch1 and Kch2 in that experiment may have been overwhelmed by those of nutritional activities Trk1 and Trk2. It will be interesting to revisit this question using cells that lack Trk1 and Trk2 or overexpress Kch1 and Kch2 combined with new probes for direct measurement of transmembrane potential (22, 23).

Kch1 and Kch2 function at the apex of death-suppressing regulatory pathway. HACS, calmodulin, and Cn are not necessary for the efficient mating of *S. cerevisiae* cells, but they are necessary for the survival of nonmating cells exposed to mating pheromones. The *kch1 kch2* double mutant died as dramatically as *cch1* mutants, and the lethal effects of mating pheromones could be rescued by the addition of high Ca^{2+} to the culture medium (Fig. 2). These experiments position Kch1 and Kch2 at the apex of the calcium signaling pathway that is used by *S. cerevisiae* cells for survival during prolonged exposures to mating pheromones.

Ca^{2+} influx through HACS and activation of Cn is also necessary for survival of *S. cerevisiae* cells exposed to compounds that stress the endoplasmic reticulum (35). These stressors include tunicamycin, dithiothreitol, and Ca^{2+} starvation, which all disrupt biogenesis and trafficking of secretory proteins and consequently activate the unfolded protein response (UPR) signaling pathway. The UPR factors Ire1 and Hac1 were not required for death-promoting effects of tunicamycin or the death-suppressing activation of HACS. Instead, the stress-responsive Slt2/Mpk1 protein kinase and many of its upstream regulators were required for HACS-dependent Ca^{2+} uptake in response to ER stressors (39). Preliminary findings suggest Kch1, rather than Kch2, responds to tunicamycin and other ER stressors and activates HACS (unpublished observations). Kch2 therefore appears to function specifically in the response to mating pheromones upon induction by the pheromone-responsive transcription factor (38).

Diverse pathogenic fungi, ranging from the yeast *Candida albicans* to the basidiomycete *Cryptococcus neoformans*, require the activation of Cn in order to survive assault with the most common class of antifungal drugs, the inhibitors of sterol biosynthesis (12). HACS has been shown to be necessary for survival of *S. cerevisiae* and *Candida glabrata* cells during exposure to azole-class compounds (18, 35, 49). Although it is not yet known whether homologs of Kch1 and Cch1 contribute to Cn activation and survival in clinically relevant situations, compounds that specifically inhibit Kch1 or HACS in fungi may augment the potency of azole-class compounds in antifungal therapies by diminishing the activation of Cn and downstream processes that are essential for fungal cell survival.

ACKNOWLEDGMENTS

This research was supported by grants GM053082 and NS074072 to K.W.C. and EY10852 and GM085335 to C.M. from the National Institutes of Health (NIH). A.R. and C.L.S. were supported by NIH grant GM60696.

We thank Alonso Rodriguez-Navarro for the *trk1 trk2* double-mutant yeast strain.

A.R. and C.L.S. performed and analyzed patch-clamp studies of yeast protoplasts. C.M. and T.S. performed and analyzed the whole-cell recording experiments on HEK293T cells. C.S., N.Z., and K.W.C. planned and performed the remaining experiments. All authors contributed to the writing and editing of the manuscript.

REFERENCES

1. **Cunningham KW.** 2011. Acidic calcium stores of *Saccharomyces cerevisiae*. Cell Calcium **50**:129–138.
2. **Iida H, Yagawa Y, Anraku Y.** 1990. Essential role for induced Ca^{2+} influx followed by $[Ca^{2+}]_i$ rise in maintaining viability of yeast cells late in the mating pheromone response pathway: a study of $[Ca^{2+}]_i$ in single *Saccharomyces cerevisiae* cells with imaging of fura-2. J. Biol. Chem. **265**:13391–13399.
3. **Sprague GF, Jr, Thorner JW.** 1992. Pheromone response and signal transduction during the mating process of *Saccharomyces cerevisiae*, p 657–744. *In* Jones EW, Pringle JR, Broach JR (ed), The molecular and cellular biology of the yeast *Saccharomyces*: gene expression. Cold Spring Harbor Laboratory Press, Cold Spring Harbor, NY.
4. **Ohsumi Y, Anraku Y.** 1985. Specific induction of Ca2+ transport activity in *MATa* cells of *Saccharomyces cerevisiae* by a mating pheromone, alpha factor. J. Biol. Chem. **260**:10482–10486.
5. **Muller EM, Locke EG, Cunningham KW.** 2001. Differential regulation of two Ca^{2+} influx systems by pheromone signaling in *Saccharomyces cerevisiae*. Genetics **159**:1527–1538.
6. **Muller EM, Mackin NA, Erdman SE, Cunningham KW.** 2003. Fig1p facilitates Ca^{2+} influx and cell fusion during mating of *Saccharomyces cerevisiae*. J. Biol. Chem. **278**:38461–38469.
7. **Cyert MS, Kunisawa R, Kaim D, Thorner J.** 1991. Yeast has homologs (*CNA1* and *CNA2* gene products) of mammalian calcineurin, a calmodulin-regulated phosphoprotein phosphatase. Proc. Natl. Acad. Sci. U. S. A. **88**:7376–7380.
8. **Cyert MS, Thorner J.** 1992. Regulatory subunit (*CNB1* gene product) of yeast Ca^{2+}/calmodulin-dependent phosphoprotein phosphatases is required for adaptation to pheromone. Mol. Cell. Biol. **12**:3460–3469.
9. **Moser MJ, Geiser JR, Davis TN.** 1996. Ca^{2+}-calmodulin promotes survival of pheromone-induced growth arrest by activation of calcineurin and Ca^{2+}-calmodulin-dependent protein kinase. Mol. Cell. Biol. **16**: 4824–4831.
10. **Fischer M, Schnell N, Chattaway J, Davies P, Dixon G, Sanders D.** 1997. The *Saccharomyces cerevisiae CCH1* gene is involved in calcium influx and mating. FEBS Lett. **419**:259–262.
11. **Paidhungat M, Garrett S.** 1997. A homolog of mammalian, voltage-gated calcium channels mediates yeast pheromone-stimulated Ca^{2+} uptake and exacerbates the *cdc1*(Ts) growth defect. Mol. Cell. Biol. **17**:6339–6347.
12. **Steinbach WJ, Reedy JL, Cramer RA, JR, Perfect JR, Heitman J.** 2007. Harnessing calcineurin as a novel anti-infective agent against invasive fungal infections. Nat. Rev. Microbiol. **5**:418–430.
13. **Iida H, Nakamura H, Ono T, Okumura MS, Anraku Y.** 1994. *MID1*, a novel *Saccharomyces cerevisiae* gene encoding a plasma membrane protein, is required for Ca^{2+} influx and mating. Mol. Cell. Biol. **14**:8259–8271.
14. **Locke EG, Bonilla M, Liang L, Takita Y, Cunningham KW.** 2000. A

homolog of voltage-gated Ca^{2+} channels stimulated by depletion of secretory Ca^{2+} in yeast. Mol. Cell. Biol. **20**:6686–6694.
15. **Martin DC, Kim H, Mackin NA, Maldonado-Baez L, Evangelista CC, Beaudry VG, Dudgeon DD, Naiman DQ, Erdman SE, Cunningham KW.** 2011. New regulators of a high-affinity Ca^{2+} influx system (HACS) revealed through a genome-wide screen in yeast. J. Biol. Chem. **286**: 10744–10754.
16. **Viladevall L, Serrano R, Ruiz A, Domenech G, Giraldo J, Barcelo A, Arino J.** 2004. Characterization of the calcium-mediated response to alkaline stress in *Saccharomyces cerevisiae.* J. Biol. Chem. **279**:43614–43624.
17. **Brand A, Shanks S, Duncan VMS, Yang M, Mackenzie K, Gow NAR.** 2007. Hyphal orientation of *Candida albicans* is regulated by a calcium-dependent mechanism. Curr. Biol. **17**:347–352.
18. **Hong MP, Vu K, Bautos J, Gelli A.** 2010. Cch1 restores intracellular Ca^{2+} in fungal cells during endoplasmic reticulum stress. J. Biol. Chem. **285**: 10951–10958.
19. **Slayman CL.** 1965. Electrical properties of *Neurospora crassa*: effects of external cations on the intracellular potential. J. Gen. Physiol. **49**:69–92.
20. **Slayman CL, Long WS, Lu CY.** 1973. The relationship between ATP and an electrogenic pump in the plasma membrane of *Neurospora crassa.* J. Membr. Biol. **14**:305–338.
21. **PeñA A, Sánchez NS, Calahorra M.** 2010. Estimation of the electric plasma membrane potential difference in yeast with fluorescent dyes: comparative study of methods. J. Bioenerg. Biomembr. **42**:419–432.
22. **Madrid R, Gómez MJ, Ramos J, Rodríguez-Navarro A.** 1998. Ectopic potassium uptake in *trk1 trk2* mutants of *Saccharomyces cerevisiae* correlates with a highly hyperpolarized membrane potential. J. Biol. Chem. **273**:14838–14844.
23. **Maresova L, Urbankova E, Gaskova D, Sychrova H.** 2006. Measurements of plasma membrane potential changes in *Saccharomyces cerevisiae* cells reveal the importance of the Tok1 channel in membrane potential maintenance. FEMS Yeast Res. **6**:1039–1046.
24. **Ko CH, Gaber RF.** 1991. TRK1 and TRK2 encode structurally related K^+ transporters in *Saccharomyces cerevisiae.* Mol. Cell. Biol. **11**:4266–4273.
25. **Bihler H, Slayman CL, Bertl A.** 2002. Low-affinity potassium uptake by *Saccharomyces cerevisiae* is mediated by NSC1, a calcium-blocked nonspecific cation channel. Biochim. Biophys. Acta **1558**:109–118.
26. **Bihler H, Slayman CL, Bertl A.** 1998. NSC1: a novel high-current inward rectifier for cations in the plasma membrane of *Saccharomyces cerevisiae.* FEBS Lett. **432**:59–64.
27. **Longtine MS, AMcKenzie, 3rd, Demarini DJ, Shah NG, Wach A, Brachat A, Philippsen P, Pringle JR.** 1998. Additional modules for versatile and economical PCR-based gene deletion and modification in *Saccharomyces cerevisiae.* Yeast **14**:953–961.
28. **Sherman F, Hicks JB, Fink GR.** 1986. Methods in yeast genetics. Cold Spring Harbor Laboratory, Cold Spring Harbor, NY.
29. **Kranz JE, Satterberg B, Elion EA.** 1994. The MAP kinase Fus3 associates with and phosphorylates the upstream signaling component Ste5. Genes Dev. **8**:313–327.
30. **Batiza AF, Schulz T, Masson PH.** 1996. Yeast respond to hypotonic shock with a calcium pulse. J. Biol. Chem. **271**:23357–23362.
31. **Mehta S, Li H, Hogan PG, Cunningham KW.** 2009. Domain architecture of the regulators of calcineurin (RCANs) and identification of a divergent RCAN in yeast. Mol. Cell. Biol. **29**:2777–2793.
32. **Cunningham KW, Fink GR.** 1994. Calcineurin-dependent growth control in *Saccharomyces cerevisiae* mutants lacking *PMC1*, a homolog of plasma membrane Ca^{2+} ATPases. J. Cell Biol. **124**:351–363.
33. **Cunningham KW, Fink GR.** 1996. Calcineurin inhibits VCX1-dependent H^+/Ca^{2+} exchange and induces Ca^{2+} ATPases in *Saccharomyces cerevisiae.* Mol. Cell. Biol. **16**:2226–2237.
34. **Bertl A, Bihler H, Reid JD, Kettner C, Slayman CL.** 1998. Physiological characterization of the yeast plasma membrane outward rectifying K^+ channel, DUK1 (TOK1), in situ. J. Membr. Biol. **162**:67–80.
35. **Bonilla M, Nastase KK, Cunningham KW.** 2002. Essential role of calcineurin in response to endoplasmic reticulum stress. EMBO J. **21**:2343–2353.
36. **Scannell DR, Frank AC, Conant GC, Byrne KP, Woolfit M, Wolfe KH.** 2007. Independent sorting-out of thousands of duplicated gene pairs in two yeast species descended from a whole-genome duplication. Proc. Natl. Acad. Sci. U. S. A. **104**:8397–8402.
37. **Roberts CJ, Nelson B, Marton MJ, Stoughton R, Meyer MR, Bennett HA, He YD, Dai H, Walker WL, Hughes TR, Tyers M, Boone C, Friend SH.** 2000. Signaling and circuitry of multiple MAPK pathways revealed by a matrix of global gene expression profiles. Science **287**:873–880.
38. **Heiman MG, Walter P.** 2000. Prm1p, a pheromone-regulated multispanning membrane protein, facilitates plasma membrane fusion during yeast mating. J. Cell Biol. **151**:719–730.
39. **Bonilla M, Cunningham KW.** 2003. Mitogen-activated protein kinase stimulation of Ca^{2+} signaling is required for survival of endoplasmic reticulum stress in yeast. Mol. Biol. Cell **14**:4296–4305.
40. **McCoy JG, Nimigean CM.** 2012. Structural correlates of selectivity and inactivation in potassium channels. Biochim. Biophys. Acta **1818**:272–285.
41. **Durell SR, Guy HR.** 1999. Structural models of the KtrB, TrkH, and Trk1,2 symporters based on the structure of the KcsA K^+ channel. Biophys. J. **77**:789–807.
42. **Ketchum KA, Joiner WJ, Sellers AJ, Kaczmarek LK, Goldstein SA.** 1995. A new family of outwardly rectifying potassium channel proteins with two pore domains in tandem. Nature **376**:690–695.
43. **Reid JD, Lukas W, Shafaatian R, Bertl A, Scheurmann-Kettner C, Guy HR, North RA.** 1996. The *Saccharomyces cerevisiae* outwardly rectifying potassium channel (DUK1) identifies a new family of channels with duplicated pore domains. Receptors Channels **4**:51–62.
44. **Saldana C, Naranjo D, Coria R, Pena A, Vaca L.** 2002. Splitting the two pore domains from TOK1 results in two cationic channels with novel functional properties. J. Biol. Chem. **277**:4797–4805.
45. **Jan LY, Jan YN.** 1990. How might the diversity of potassium channels be generated? Trends Neurosci. **13**:415–419.
46. **Mendoza I, Rubio F, Rodriguez-Navarro A, Pardo JM.** 1994. The protein phosphatase calcineurin is essential for NaCl tolerance of *Saccharomyces cerevisiae.* J. Biol. Chem. **269**:8792–8796.
47. **Catterall WA.** 2010. Ion channel voltage sensors: structure, function, and pathophysiology. Neuron **67**:915–928.
48. **Wang H, Liang Y, Zhang B, Zheng W, Xing L, Li M.** 2011. Alkaline stress triggers an immediate calcium fluctuation in *Candida albicans* mediated by Rim101p and Crz1p transcription factors. FEMS Yeast Res. **11**:430–439.
49. **Kaur R, Castaño I, Cormack BP.** 2004. Functional genomic analysis of fluconazole susceptibility in the pathogenic yeast *Candida glabrata*: roles of calcium signaling and mitochondria. Antimicrob. Agents Chemother. **48**:1600–1613.
50. **Zhang NN, Dudgeon DD, Paliwal S, Levchenko A, Grote E, Cunningham KW.** 2006. Multiple signaling pathways regulate yeast cell death during the response to mating pheromones. Mol. Biol. Cell **17**:3409–3422.
51. **Jin H, Carlile C, Nolan S, Grote E.** 2004. Prm1 prevents contact-dependent lysis of yeast mating pairs. Eukaryot. Cell **3**:1664–1673.